SERS Detection of Bacteria in Water by in Situ Coating with Ag Nanoparticles

ARTICLE *in* ANALYTICAL CHEMISTRY · JANUARY 2014

Impact Factor: 5.64 · DOI: 10.1021/ac402935p · Source: PubMed

6 AUTHORS, INCLUDING:

Danting Yang
Zhejiang University
14 PUBLICATIONS **136** CITATIONS
SEE PROFILE

Nicoleta Elena Mircescu
National Institute for Research and Developm…
12 PUBLICATIONS **90** CITATIONS
SEE PROFILE

Reinhard Niessner
Technische Universität München
595 PUBLICATIONS **12,248** CITATIONS
SEE PROFILE

Christoph Haisch
Technische Universität München
79 PUBLICATIONS **1,258** CITATIONS
SEE PROFILE

analytical chemistry

Article

pubs.acs.org/ac

SERS Detection of Bacteria in Water by in Situ Coating with Ag Nanoparticles

Haibo Zhou,[†] Danting Yang,[†] Natalia P. Ivleva,[†] Nicoleta E. Mircescu,[†,‡] Reinhard Niessner,[†] and Christoph Haisch*[,†]

[†]Institute of Hydrochemistry and Chair for Analytical Chemistry, Technische Universität München, Marchioninistraße 17, D-81377 Munich, Germany

[‡]Faculty of Physics, Babeş-Bolyai University, Kogălniceanu 1, 400084 Cluj-Napoca, Romania

Supporting Information

ABSTRACT: The bio-sensing for the convenient detection of bacteria has been widely explored with the use of various sensing materials and techniques. It is still a challenge to achieve an ultrasensitive and selective, but simple, rapid, and inexpensive detection method for bacteria. We report on surface-enhanced Raman scattering (SERS) for the detection of living bacteria in drinking water by employing a synthesis of silver nanoparticles coating the cell wall of bacteria. We found that the Raman signals intensity of bacteria after AgNP synthesis mainly depends on the zeta potential of the cell wall. The enhancement of the Raman signal of bacteria using this strategy is about 30-fold higher than that in the case of a simply mixed colloid−bacterial suspension. The total assay time required is only 10 min and the total reactants' volume needed to analyze bacteria in a real environment is as low as 1 mL. Particularly, only one droplet of 3 μL sample is necessary for each SERS measurement. Furthermore, we can use this novel strategy to discriminate three strains of *Escherichia coli* and one strain of *Staphylococcus epidermidis* by hierarchy cluster analysis. Finally, we can detect bacteria down to 2.5×10^2 cells/mL on a hydrophobic glass slide by SERS mapping. Thus, our detection method offers prominent advantages, such as reduced assay time, simple handling, low reactant volumes, small amount of sample, and higher sensitivity and selectivity compared to previously reported label free methods. This novel strategy may be extended to open an avenue for developing various SERS-based biosensors.

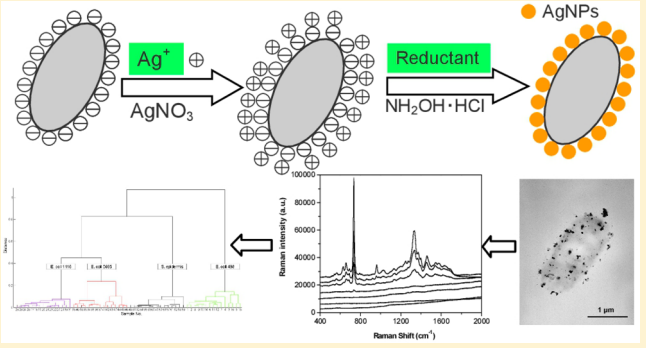

Accurate and sensitive detection of microorganisms, such as *Escherichia coli* (*E. coli*), *Legionella pneumophila*, *Salmonella typhimurium*, and other waterborne and foodborne pathogens in water and food are critical for food safety and human health care.[1,2] The main reason is that many serious and even fatal diseases are caused by bacterial infections or contaminations.[3] Rapid and sensitive detection can prevent and control pathogen-related diseases and potential bioterrorism attacks.[4] In the last century, standard methods for microorganism detection, such as plating and culturing, were established and further optimized. These methods are sensitive and selective, but exceedingly time-consuming due to the fact that they rely on several enrichment steps.[5,6] In addition, a number of methods, including flow cytometry,[7] enzyme-linked immunosorbent assay (ELISA),[8] and polymerase chain reaction (PCR)[9] have been developed. However, these methodologies are limited in regards to sensitivity, specificity, speed, cost efficiency, versatility, or throughput for routine low level bacteria detection.[10]

Since the discovery that Raman signals are enhanced at rough silver electrode surface,[11−13] SERS has become a subject of interest for the detection of chemicals,[14,15] biological species,[16] for molecular imaging, and for monitoring microorganisms,[17] cells,[18] and tissues,[19] even in vivo.[20] The main reasons are its high sensitivity, intrinsic selectivity due to the spectroscopic fingerprint, simple and fast preparation, and nondestructive data acquisition in aqueous environment. In particular, the detection and identification of microorganisms by SERS has attracted interest recently, motivated by the potential application on single whole microorganisms.[2,21,22] The enhancement is generally attributed to the electromagnetic field in the proximity of nanostructured metal surfaces.[14] In recent bacterial SERS experiments, mostly suspensions of either colloidal gold (AuNPs) or silver nanoparticles (AgNPs) of various shapes or particle aggregates, induced by inorganic salt, were employed to generate the SERS effect by simply mixing with the bacterial cells.[23] The SERS-based bioanalysis is considered label-free, because it does not require for a specific detection label, such as a fluorescence or chemiluminescence dye, which makes it easier and faster.[24,25]

Received: September 20, 2013
Accepted: January 3, 2014
Published: January 3, 2014

   dx.doi.org/10.1021/ac402935p | *Anal. Chem.* 2014, 86, 1525−1533

As mentioned previously, simple mixing is a common approach for SERS detection of bacteria. However, the generated mixture is not always homogeneous.[26,27] There are no specific interactions between the bacteria and NPs. Additionally, the capping reagent employed for stabilizing the NPs prohibits intimate contact with bacteria. The inefficient interaction of NPs with the bacterial cell wall resulted in a very limited reproducibility of bacterial SERS spectra. This limitation can be overcome either by increasing the NP concentration[23,28] or by the "convective assembly" method,[29] but these methods often have poor reproducibility due to the difficulty posed by efficient, precise control of the NP aggregation process on the bacteria. Thus, the main goal is that the NPs could come into contact with the bacteria surface at as many points and close as possible.[23]

Recently, an electrostatic attraction force strategy for efficient, precise self-assembly NPs on bacteria has been developed.[21,30,31] The fact is based on that the bacteria wall is negatively charged for the presence of either teichoic acid in Gram-positive bacteria,[30] or the outer membrane lipopolysaccharides in Gram-negative bacteria.[32] The positive charged poly (L-lysine) coated AuNPs,[31] cetyltrimethylammonium bromide (CTAB)-terminated nanorods[30] and poly(allylamine hydrochloride) (PAH)/AuNPs/PAH layer by layer (LbL) structures[21] can allow the highly efficient and precise deposit onto the bacterial cell wall through electrostatic interaction. However, all these methods have either a complicated procedure or fail to provide reliable results for real samples, no actual SERS experiments are realized; furthermore, they probably have the potential to create interfering SERS signals of the capping reagents.[21]

Therefore, there has always been a strong driving force to develop a rapid, simple, and efficient method to deposit NPs on the bacterial cell wall for SERS application. Until now, Efrima's group has developed a method to directly produce NPs in the presence of the bacteria.[33−36] They can direct the production of the NPs to either intimate contact at external (cell wall) or interior components of bacteria.[36] Although this procedure ensures an intimate contact of the colloids with the cell, the authors obtained very similar spectra for different species of silver-coated bacteria, which makes the method unsuitable for bacteria discrimination. Furthermore, they do not deeply discuss the formation mechanism and the direct influence of this synthesis methodology. A literature survey shows that there is only one additional paper from another group concerning in situ preparation of NPs on the surface of bacteria for SERS application.[22] So, in addition to a more straightforward and efficient synthesis of NPs on the surface of bacteria for SERS application in real-world samples, a more clear interaction mechanism of the NPs with bacteria should also be addressed.

Here, we report an in situ synthesis of AgNP coating on the cell wall of bacteria for SERS-based label free detection of bacteria in drinking water, which is a more efficient way to achieve intimate contact between NPs and the bacteria cell in comparison to previous methods. We first soaked bacteria in a silver nitrate solution and then used hydroxylamine hydrochloride as a reducing agent. Finally, a "colloid deposit" was formed on the cell wall of the bacteria, which is addressed in the following as "Bacteria@AgNP".

EXPERIMENTAL SECTION

Chemicals, Biochemicals, and Materials. Methanol, ethanol, 25% ammonia (NH_4OH), 98% sulfuric acid (H_2SO_4), 37% hydrochloric acid (HCl), sodium hydroxide (NaOH), sodium choride (NaCl), hydroxylamine hydrochloride ($NH_2OH{\cdot}HCl$), silver nitrate ($AgNO_3$), and trimethoxy-(propyl)silane ($CH_3CH_2CH_2Si(OCH_3)_3$) were purchased from Sigma-Aldrich (Taufkirchen, Germany) and used without further purification. *E. coli DSM 498/1116/5695* shock frozen strains were purchased from DSM nutritional products (Grenzach, Germany). *Staphylococcus epidermidis 61741* (*S. epidermidis*) was supported by Max-von-Pettenkofer-Institute, Ludwig-Maximilians-University. Glass slides (26 mm × 76 mm × 1 mm) were purchased from Carl Roth (Karlsruhe, Germany). Activation of glass slides, cleaning steps, and the hydrophobic procedure were performed in plastic containers from Carl Roth. Hellmanex solution was purchased from Hellma (Muellheim, Germany). Milli-Q water (18.2 MΩ cm) was produced using a Millipore water purification system.

Phosphate buffered saline (PBS, pH = 7.6, 200 mM) contained 3.40 g (25 mM) KH_2PO_4, 30.50 g (175 mM) K_2HPO_4, and 21.25 g NaCl (362.5 mM) in 1 L Milli-Q water and was filtered before use. The other concentrations of PBS (0.1, 1, 10, 80, 100 mM) were diluted from this bulk PBS buffer (200 mM).

Microorganism Preparation. Shock-frozen *E. coli DSM 498/1116/5695* cells were cultivated in LB medium (Lennox) (100 mL in 250 mL flasks) in a gyratory shaker at 100 rpm and 37 °C for 16 h. Ten milliliters of bacteria were harvested and washed twice in H_2O ("Bacteria(H_2O)") or PBS ("Bacteria(PBS)") by centrifugation at 4500 rpm and 4 °C. Then the bacteria were stored in refrigerator at 4 °C for further use. *S. epidermidis 61741* was obtained from the strain collection of the Max-von-Pettenkofer-Institute, Ludwig-Maximilians-University. Prior to analysis, all cell suspensions were diluted in PBS or H_2O to reach the desired concentrations. The stock cell concentration of *E. coli* was determined by flow-cytometry using SYTO9.

Zeta Potential Measurement. The zeta potential of *E. coli DSM 1116* in water and PBS was measured by dynamic light scattering with Zetasizer Nano ZS (Malvern Instrument Ltd. Worcestershire, UK), equipped with a glass electrophoresis cell. The concentrations of *E. coli DSM 1116* were 1×10^8 cell/mL; no pH adjustment was carried out. These parameters were consistent for all the following reported measurements.

Glass Slide Hydrophobic Treatments. *Cleaning.* The normal glass slides were put in a chip reservoir containing a 2% Hellmanex solution and left for 1 h in an ultrasonic bath to rinse. Subsequently, the chips were put on a shaker overnight (15 h) at room temperature followed by 1 h in an ultrasonic bath. The treated slides were thoroughly washed five times in 200 mL Milli-Q water and dried under nitrogen flow. The prepared glass slides were dipped in 200 mL of methanol/hydrochloric acid solution (1:1) and left shaking for 1 h at room temperature. A washing step in water followed, where the chips were rinsed five times in 200 mL Milli-Q water. Subsequently, they were submerged in concentrated sulfuric acid and left shaking for 1 h at room temperature. An additional washing step in water followed and the slides were again dried under a nitrogen flow.[37]

Hydrophobic Treatment. The cleaned slides were put in a chip reservoir containing a 150 mL methanol and 150 mL water mixed solution under magnetic stirring, then 2 mL of trimethoxy(propyl)silane was added dropwise followed by addition of 3 mL of 25% ammonia. The solution was stirred overnight. Finally, the chips were thoroughly washed five times in 300 mL of absolute ethanol and the slides were again dried under a nitrogen flow.[38]

Colloid Synthesis. *Conventional Silver Nanoparticle (AgNP) Preparation.* As a reference, standard AgNPs were synthesized as used in earlier experiments.[39−41] The preparation

dx.doi.org/10.1021/ac402935p | Anal. Chem. 2014, 86, 1525−1533

follows a modified procedure of Leopold and Lendl.[42,43] Briefly, 17 mg (0.1 mmol) of $AgNO_3$ was dissolved in Milli-Q water (10 mL). One-hundred milliliters of 11.6 mg (0.17 mmol) $NH_2OH{\cdot}HCl$ solution containing 3.3 mL of NaOH (0.1 M) was prepared and divided in 9 mL batches in centrifuge tubes. To the reducing agent was added 1 mL of $AgNO_3$ in a flow rate of 0.67 mL s^{-1} without stirring. Finally, the centrifuge tube was inverted once to complete the mixing. The size distribution of silver colloid suspension was tested using a UV−vis spectrometer and TEM (procedure details are described later). The yellow/greenish colloid sols were stored in the dark at 4 °C.

Bacteria−AgNP. A 1 mL sample liquid was centrifuged at 4500 rpm, and the supernatant was discarded. The resulting mixture was further added to 1 mL of prepared AgNPs, and the mixture vortexed to ensure homogeneity. Subsequently, we pipetted 10 μL of 1 M NaCl into the prepared mixture as an agglomerating agent. The final concentration of NaCl was 0.01 M. The resulting hybrid bacterial suspension is designated as "Bacteria−AgNP".

Bacteria@AgNP. Again, a 1mL sample liquid was centrifuged at 4500 rpm, and the supernatant was discarded. Then 100 μL of 10 mM $AgNO_3$ solution was added, and the mixture was vortexed and then an interaction time of 5 min was allowed. Subsequently, 900 μL of $NH_2OH{\cdot}HCl$ solution was pipetted into the prepared mixture and the mixture was again vigorously vortexed. Finally, we stored the suspension in the dark at 4 °C until it was analyzed. The resulting hybrid bacterial suspension is designated as Bacteria@AgNP. In detail, the water-washed *E. coli* are called "Bacteria(H_2O)@AgNP", and the different concentrations of PBS-washed *E. coli* are called "Bacteria(PBS)@AgNP". The same procedure was used for *S. epidermidis*.

SERS Measurements. *SERS Detection of Bacteria in Suspension.* 3 μL of the sample suspension, already treated with the different colloid preparations, was pipetted onto the normal glass slides. The recording of the Raman spectra was started right after this sample preparation, using the 633 nm line of a He−Ne with 14 mW power at the sample and a 10× objective. The Raman spectra were continuously (one spectrum every 40 s) collected with the auto repeat function until the droplet was dried. If not explicitly stated, the exposure time was 1 s and the number of accumulations was 10, and the confocal slit width was 100 μm, detecting a spectral region of 50−3000 cm^{-1}.

SERS Mapping on Glass Slides. A droplet of 3 μL of the sample suspension was added on the hydrophobic glass slides and then dried at room temperature. If not explicitly stated, all SERS mapping data were obtained by using the 633 nm He−Ne laser line with 1.4 mW power and a 50× objective. The exposure time and the accumulation number were 1 s and 5, respectively; the slit width was 100 μm, detecting spectra region of 50−2000 cm^{-1}. The mapping area is 40 × 40 μm^2 with step size of 2 μm. In all, 441 Raman spectra were collected for each map.

Colloid Diagnostics. UV−vis absorption spectra were recorded with a Specord Plus spectrometer (Analytik Jena, Jena, Germany). All of the UV−vis spectra in suspension were obtained at room temperature using water as solvent with a path length of 1 cm. ICP-MS analyses were carried out by a Perkin-Elmer SCIEX ELAN 6100 (PerkinElmer Inc., Waltham, USA). TEM images were taken with JEM 2010 (JEOL, Munich, Germany) with an accelerating voltage of 200 kV. SERS measurements were conducted with a Raman microscope (LabRAM HR, HORIBA Scientific, Japan).

RESULTS AND DISCUSSION

Dynamic SERS. For the analysis, a new SERS detection method was used. It is called dynamic surface-enhancement Raman spectroscopy and has been demonstrated to enhance the signals of analytes in comparison to the traditional methods by several orders of magnitude.[44,45] The approach is straightforward and reliable: right after dropping 3 μL of Bacteria@AgNP solution on the glass slides, Raman spectra are recorded continuously at an interval of 40 s until the droplet is dried. In the course of the droplet drying, the SERS signal of the bacteria gradually increases, with the 17th spectrum (after ∼680 s) reproducibly yielding the highest intensity. Afterward, the signal suddenly decreases and fluorescent background noise appears after the water evaporation was completed (see Figure S1 in the Supporting Information). A tentative explanation of this phenomenon could be that the interparticle distance of Bacteria@AgNP becomes reduced due to the capillary force during solvent vaporization. During the initial drying, which leads to droplet shrinking, a great number of hot spots are generated by the decreasing interparticle distance of Bacteria@AgNP, which drives the initially separated Bacteria@AgNP nanostructures to self-assemble into clusters. However, cluster growth is limited by the increasing electrostatic repulsion of the cluster. The equilibrium short-range attraction and long-range Coulomb repulsion determines a finite aggregation number.[44] At the final stage, when the droplet is dried, the hot spots disappear; probably due to the formation of very big clusters.[41] The Raman results obtained by using this approach are highly reproducible and reliable. The reproducibility of this dynamic SERS approach for bacteria characterization, based on the evaluation of the seventeenth spectrum, is demonstrated by the analysis five different sample batches of 1 × 10^8 cell/mL *E. coli DSM 1116* (water-washed, see Figure S2 in the Supporting Information).

Colloid Assessment. Figure 1 illustrates the in situ formation of a AgNP coating on the cell wall of bacteria. The

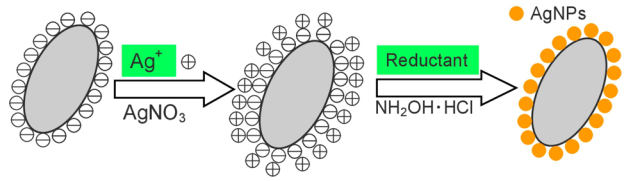

Figure 1. Schema of the in situ synthesis of nanoparticles on the bacterial surface. The silver ions adsorbed to the bacterial cell wall by electrostatic attraction generate AgNPs on the surface of bacteria immediately after the addition of the reducing reagent.

resulting complexes are then detected by SERS. The bacteria wall is negatively charged due to the presence of either teichoic acid in Gram-positive bacteria[30] or the outer membrane lipopolysaccharides in Gram-negative bacteria.[32] Hence, the silver ions strongly adhere to the bacterial cell wall by electrostatic interaction. Silver ions can also be attached to various electron-rich binding sites of nitrogen, sulfur, or carboxylate on the cell wall of bacteria via coordination force.[33] Finally, the addition of hydroxylamine hydrochloride led to the formation of colloid deposits on the surface of bacteria (Bacteria@AgNP). From the TEM images, it can be clearly seen that the AgNPs were successfully synthesized around the bacterial cell wall (see Figure 3).

The negative charge of the bacterial surface can be affected by a number of parameters, such as pH-values, ionic strength, and the

dx.doi.org/10.1021/ac402935p | Anal. Chem. 2014, 86, 1525−1533

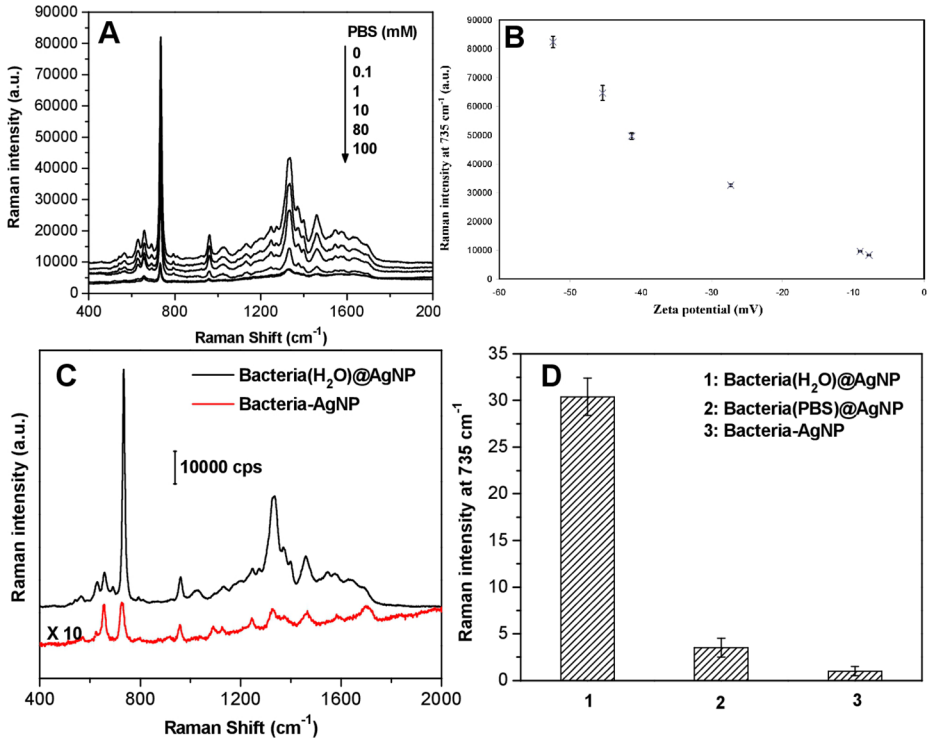

Figure 2. (A) SERS spectra 1×10^8 cell/mL *E. coli DSM 1116* Bacteria(PBS)@AgNP, washed with different concentrations of PBS. The concentrations of PBS are 0, 0.1, 1.0, 10, 80, and 100 mM, respectively. (B) Raman intensity at 735 cm^{-1} vs zeta potential of the bacteria washed with different concentrations of PBS. (C) SERS spectra of bacteria obtained by two different methods. (D) Raman intensity at 735 cm^{-1} for Bacteria(H_2O)@AgNP (0 mM PBS), Bacteria(PBS)@AgNP (80 mM PBS), and Bacteria−AgNP. Each sample was measured three times.

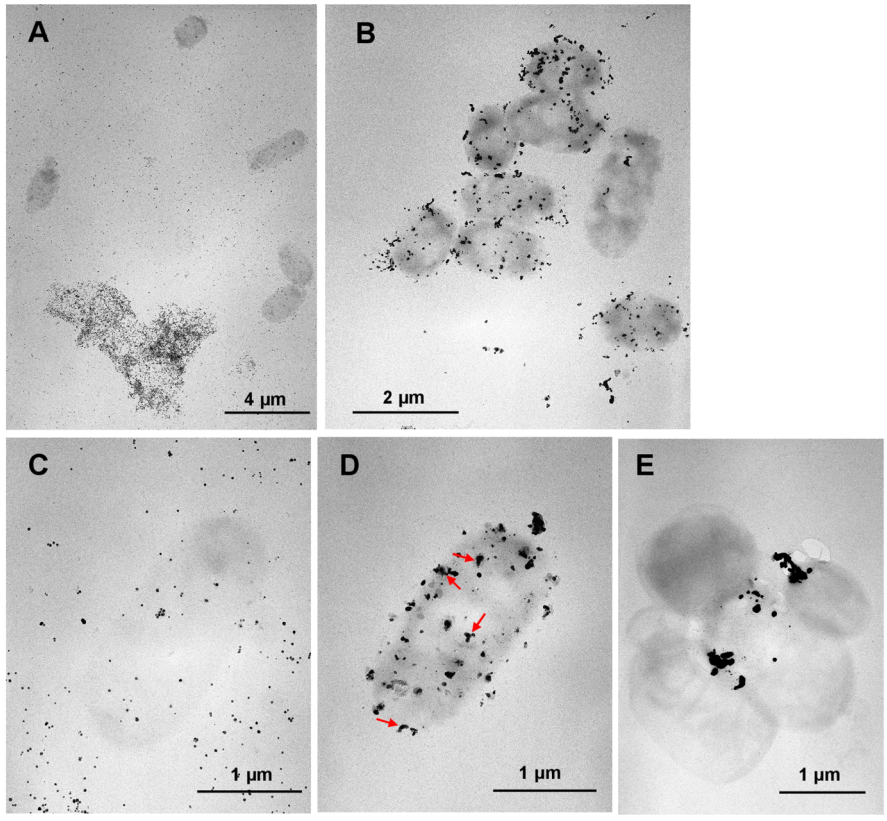

Figure 3. (A) TEM image of *E. coli DSM 1116* mixed with AgNPs and 0.01 M NaCl (Bacteria−AgNP). (B) TEM image of Bacteria(H_2O)@AgNP sample. (C), (D) High-magnification TEM images of (A) and (B), respectively. (E) TEM image of Bacteria(PBS)@AgNP nanostructures (80 mM PBS).

dx.doi.org/10.1021/ac402935p | *Anal. Chem.* 2014, 86, 1525−1533

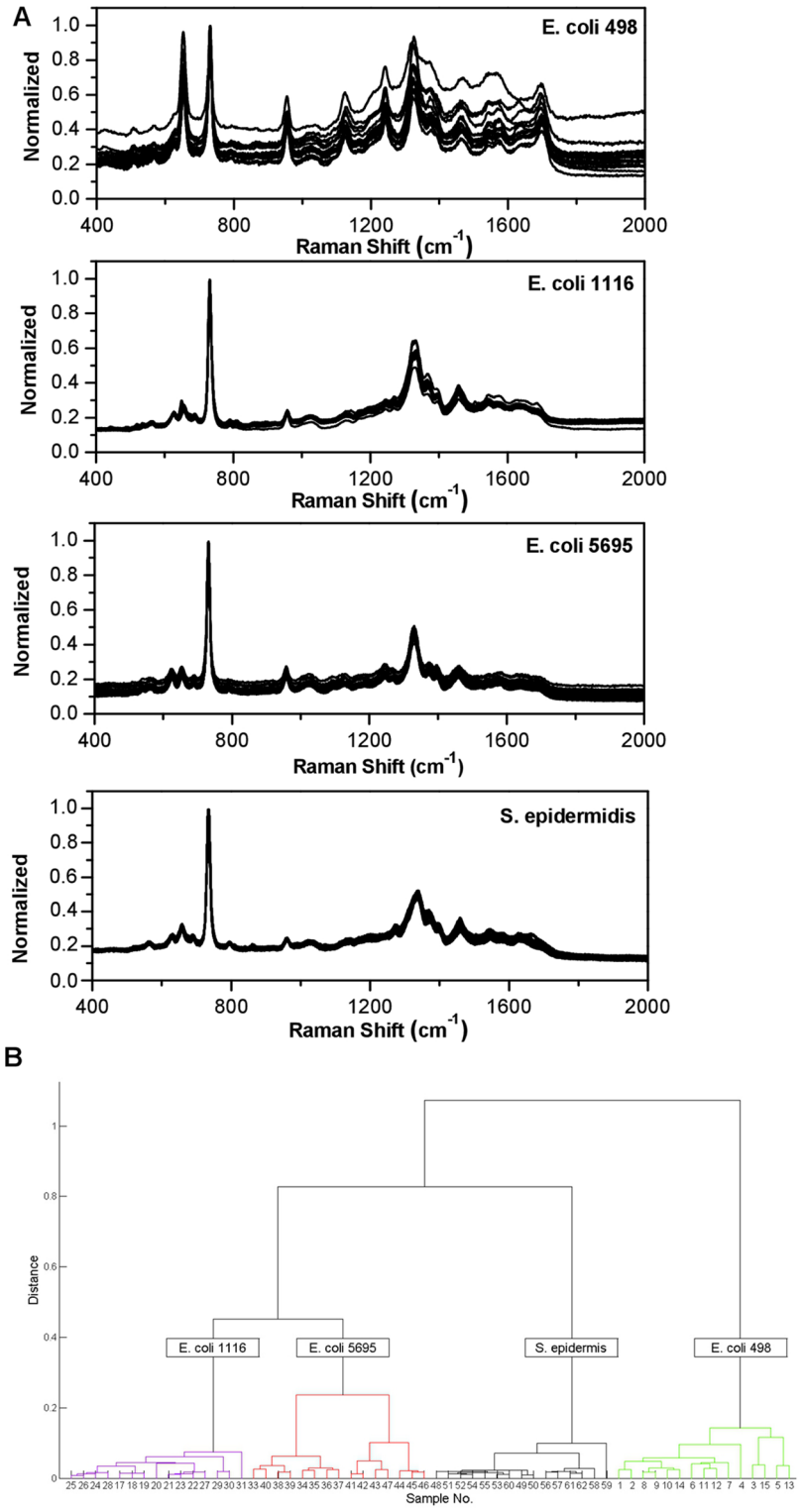

Figure 4. (A) SERS spectra of three strains of *E. coli DSM* (*498*/*1116*/*5695*) and *S. epidermidis 61741* by using Bacteria(H_2O)@AgNP synthesis. Each strain is represented in 15 spectra, acquired from 15 different batches of samples. (B) Composite dendrogram generated by hierarchy cluster analysis (HCA) from (A).

concentration of surfactants in the suspending medium.[46] To assess the surface negative charge of bacteria, the bacteria were washed with different concentrations of PBS buffer; *E. coli DSM 1116* was selected as the model bacteria. First, we prepared different concentrations of PBS solution, e.g., 0, 0.1, 1.0, 10, 80, 100 mM. Second, we used these prepared PBS solution to wash 1 × 10^8 cell/mL *E. coli DSM 1116* twice. Finally, we used these washed bacteria to measure the corresponding zeta potential and to prepare different Bacteria(PBS)@AgNP samples and then measured the corresponding Raman spectra. As shown in Figure 2A,B, when the concentrations of PBS increased, the zeta potential of the cell walls became less negative, which is

dx.doi.org/10.1021/ac402935p | *Anal. Chem.* 2014, 86, 1525−1533

consistent with the previously reported results.[46] Corresponding, the SERS signals of bacteria decrease.

For example, the zeta potential of living *E. coli DSM 1116* (1×10^8 cell/mL) in water (−52.4 mV) is about 6 times higher than the one in 80 mM PBS (−9.03 mV) (Figures 2B and S3 (Supporting Information)). Correspondingly, the enhancement by Bacteria(H_2O)@AgNP (0 mM PBS) is 9 ± 1 times higher than the one of Bacteria(PBS)@AgNP (80 mM PBS), as assessed by the strongest vibrational band at 735 cm^{-1} (Figure 2D). The surface charge of the bacteria in water is more negative than in PBS, which means that the surface of bacteria in water can adsorb more positive silver ions. Thus, more AgNPs will be synthesized on the surface of bacteria in aqueous suspension (see Figure 3D,E) and higher SERS signals of bacteria will be acquired. The enhancement effects of the Bacteria@AgNP method were further compared with the simply mixed colloid−bacterial suspension (Bacteria−AgNP). As it can be appreciated from Figure 2C and 2D, the Bacteria(H_2O)@AgNP reveal Raman intensities about 30 ± 2 times higher than the one of the Bacteria−AgNP.

A UV−vis spectroscopy characterization and TEM examination of the Bacteria@AgNP were carried out. As shown in Figure S4 (Supporting Information), no distinct peaks can be observed from the *E. coli DSM 1116* solution. The conventional AgNPs are displayed as yellow/greenish suspension and have a narrow absorption peak at 402 nm, indicating monodisperse particles with a diameter ∼30 nm (see the TEM image in Figure S5 (Supporting Information)). The Bacteria−AgNP displays a similar main peak as the AgNPs, except that the peaks width became a little larger and a broad absorption at 600−700 nm shows up, which can be explained by the aggregation of AgNPs by 0.01 M NaCl. The UV−vis spectra of Bacteria@AgNP feature a very wide absorption band at 418 nm, which is obviously red-shifted compared to the one of the Bacteria−AgNP suspension. The red shift indicates that the interparticle distance decreases and/or the size of NPs increases. All these results indicate that the AgNPs have a different morphology and show different aggregation or assembly behavior in the Bacterial@AgNP.

Subsequently, TEM analysis was performed to further investigate the morphology of the nanostructures and the distribution of AgNPs. Figure 3A depicts the TEM image of 1×10^8 cell/mL *E. coli DSM 1116* mixed with AgNPs and 0.01 M NaCl. It can be seen that the AgNPs are randomly distributed in the solution and do not aggregate on the surface of the bacteria. Some of them are self-aggregated in the suspension owing to the aggregation reagent NaCl, but they do not adhere to the bacterial surface. The bacteria remain mostly separated. The magnified image (Figure 3C) reveals that the AgNPs do not intimately adhere to the cell wall of bacteria. Consequently, the cross section of the cell wall components cannot be efficiently amplified by electromagnetic field enhancement and the SERS signals of bacteria are weak. Figure 3B,D reveals the intimate interaction of Bacteria(H_2O)@AgNP with the cell walls. Most of the particles coat the bacterial surface, whereas only a few are found unbound or clustered in the liquid phase. Figure 3D shows the high-magnification TEM image of the Bacteria(H_2O)@AgNP structures. The shape of the AgNPs is irregular, with the diameter of about 100 nm, higher than the AgNPs in Bacteria−AgNP (30 nm). Some of the composites show larger, elongated structures (indicated with red arrows in Figure 3D), which seem to be aggregated spontaneously, forming AgNPs cluster on the surface of the bacteria. Moreover, most of the bacteria were assembled in clusters under these conditions, generating more hot spots on the interfaces of bacteria and, consequently, stronger Raman signals. However, when bacteria were washed with 80 mM PBS, the Bacteria(PBS)@AgNP nanostructures were very different from Bacteria(H_2O)@AgNP. From Figure 3E, we can see that there are only few relatively large AgNPs aggregates, coating only small part of the cell wall. Most parts of bacterial cell wall are free of AgNPs. Comparing Figure 3D,E, it can be seen that there are more AgNPs coating the water-washed cell than coating the PBS-washed. The formation of few relatively large AgNPs aggregates in Bacteria(PBS)@AgNP samples can be explained by a less negative zeta potential of cell wall in consequence of the PBS washing. Furthermore, some anions, such as Cl^- (from PBS), can stimulate the formation of big AgNPs aggregated on cell wall. All of these results confirm that the SERS signal intensities of the bacteria after AgNPs synthesis mainly depends on the zeta potential of cell wall.

We found that about 96% Ag^+ was reduced onto the water-washed cell wall by ICP-MS (see discussion and Figure S6 and Table S1 in the Supporting Information). Furthermore, we can see that the sediment exhibits strong SERS signals whereas the supernatant only exhibits weak bacteria signals (see Figures S7 and S8 in the Supporting Information). These results confirm that the SERS signals of the bacteria originate from the AgNPs attached onto the cell wall, whereas the free AgNPs in suspension contribute only to a small amount to the overall SERS signals.

Bulk Liquid Bacteria Detection. The Bacteria(H_2O)@AgNP synthesis provides a highly sensitive and reproducible SERS method of bacteria detection. Figure S9 (Supporting Information) shows SERS spectra of different liquid phase number concentrations of *E. coli DSM 1116*, obtained by using the Bacteria(H_2O)@AgNP synthesis. The intensity of the SERS signals of bacteria obviously scales with the bacteria concentration (1×10^3 to 1×10^8 cell/mL). A calibration curve is given in Figure S10 (Supporting Information). Down to a level of 1×10^3 cell/mL, the strongest band at 735 cm^{-1} can be clearly detected (the red circle in Figure S10 (Supporting Information)). These results confirm that this strategy exhibits a huge Raman enhancement effect on the component of cell wall of *E. coli*, such as polysaccharides, amino acids, nucleic acid, lipids, and proteins. The typical Raman peaks at 624, 652, 735, 955, 1330, and 1456 cm^{-1} are observed (see the detailed tentative assignments of peaks in Table S2 in the Supporting Information).

To investigate the potential of this strategy to discriminate between bacteria on strain level by SERS, three strains of *E. coli DSM (498/1116/5695)* and one strain of *S. epidermidis 61741* were selected as a model. The SERS spectra in Figure 4A show the Raman results of three strains of *E. coli* and one strain of *S. epidermidis* from 60 batches of samples (each strain was represented by 15 batches, sample Nos. 1−15 belonging to *E. coli 498*, Nos. 17−31 to *E. coli 1116*, Nos. 33−47 to *E. coli 5695*, Nos. 48−62 to *S. epidermidis*). For clarity, all the SERS spectra have been normalized. The SERS spectra of the three strains of *E. coli* and *S. epidermidis* exhibit only minor differences (see Figure S11 in the Supporting Information), because the cell walls of these *E. coli* strains and *S. epidermidis* essentially have the same components. However, we can discriminate the three strains of *E. coli* and *S. epidermidis* by hierarchy cluster analysis (HCA), which was performed in Matlab.[26] All spectra were normalized to a range from 0 to 1. A composite dendrogram derived from HCA was used for statistical analysis. The resultant dendrogram shows clear characterization at strain level for each of the strains analyzed (Figure 4B).

dx.doi.org/10.1021/ac402935p | *Anal. Chem.* 2014, 86, 1525−1533

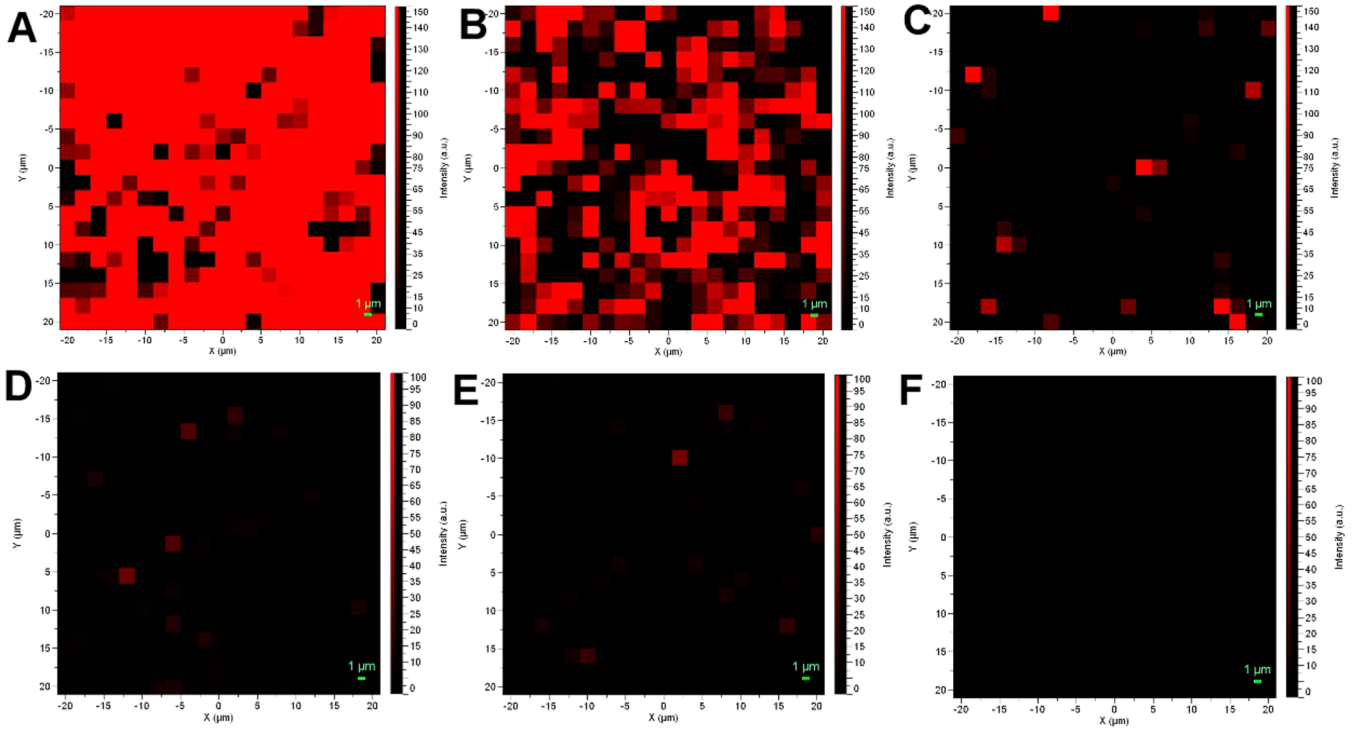

Figure 5. SERS mapping of different concentrations water-washed *E. coli DSM 1116* (Bacteria(H_2O)@AgNP) on hydrophobic glass slides. The concentrations are 1×10^7 (A), 1×10^6 (B), 1×10^5 (C), 1×10^4 (D), 1×10^3 (E), and 1×10^2 cell/mL (F), respectively (λ_{ex} = 633 nm, the exposure time was 1 s and the number of accumulations 5, objective 50×, step size 2 μm, mapping area: 21 × 21 = 441 points).

Detection of Bacteria on a Chip Surface. We evaluated the performance of our new in situ generated SERS colloids for the detecting bacteria not only in a bulk liquid but also on surfaces. SERS mapping experiments on Bacteria(H_2O)@AgNP (1×10^8 cell/mL *E. coli* DSM *1116*) were carried out on normal untreated glass slides as used in previous reports[38] and hydrophobic glass slides. One merit of a hydrophobic surface is that it substantially reduces the contact area between the droplet and the underlying surface in comparison to the hydrophilic one. Thus, the analyte present in the droplet gets higher concentrated by the liquid evaporation on the hydrophobic surface. This is known as the hydrophobic condensation effect, which further increases the SERS signals.[47] We dropped a volume (3 μL) of Bacteria(H_2O)@AgNP sample each on normal and hydrophobic glass slides, respectively. As the images show in Figure S12 (Supporting Information), the droplet on the hydrophobic glass slide is much smaller; after the drying of the sample solution, again the area of sample distribution is smaller than that of on the normal glass slides, resulting in higher bacteria concentrations on the surface. The optical images in Figure S13 (Supporting Information) confirm this conclusion. From Figure S13 (Supporting Information), it can be clearly seen that the distribution of bacteria on normal glass slides is disperse; only a few bacteria are present on the selected area (40 × 40 μm). In contrast, there is a considerable amount of bacteria on the hydrophobic surface of the same area, and the bacteria are densely assembled to the thin bacterial film at the concentration of 1×10^8 cell/mL.

Finally, the homogeneity of the substrate was investigated by SERS mapping. The SERS map shown in Figure S14 (Supporting Information) was obtained with a 2 μm step size, covering an area of 40 × 40 μm^2 (see the details of SERS mapping parameters in the Experimental Section). Surface coverage of the bacteria was analyzed using these maps, which was quantified by using the area of the strongest peak at 735 cm^{-1}. Figure S14 (Supporting Information) shows typical SERS mapping images of Bacteria(H_2O)@AgNP (1×10^8 cell/mL *E. coli DSM 1116*) on two kinds of glass slides. Each red spot represents the bacteria SERS signal detected, and the black spot means that no signal of bacteria was obtained. The signals intensities vary due to the bacteria partial inhomogeneous coverage on the glass slides or the variations in the number of AgNPs around the surface of single bacterium. From Figure S14 (Supporting Information), it can be clearly seen that the SERS signals of bacteria distribution on hydrophobic surface are more homogeneous and the number of bacteria is higher, although identical volumes and concentrations were used for both tests. Therefore, the following experiments of SERS mapping were assessed on the hydrophobic glass slides.

This spatially resolved mapping analysis of bacteria was further used to detect different concentrations of *E. coli DSM 1116* (water-washed) in drinking water. Figure 5 shows SERS mapping images of different concentrations of *E. coli DSM 1116* obtained by using the Bacteria(H_2O)@AgNP synthesis. As presented in Figure S15 (Supporting Information), the number of red dots, i.e., the number of bacteria bound to the surface, corresponds to the total concentration of bacteria. The data employed for this evaluation is discussed in detail elsewhere.[39] From Figure S15 (Supporting Information), a LOD of 2.5 × 10^2 cell/mL and dynamic range up to 1×10^8 cell/mL can be calculated.

■ CONCLUSIONS

In this work, we presented an in situ synthesis of AgNPs on the cell wall of bacteria (Bacteria@AgNP) for label-free SERS detection of bacteria in drinking water. Bacteria@AgNP has been generated successfully, resulting in highly sensitive bacteria

dx.doi.org/10.1021/ac402935p | *Anal. Chem.* 2014, 86, 1525−1533

detection. It was found that the SERS signals of bacteria measured by this method mainly depends on the zeta potential of the cell wall. The enhancement effect of the SERS signal when using the Bacteria(H_2O)@AgNP is about 9 times higher than the one for Bacteria(PBS)@AgNP (80 mM PBS) and about 30-fold higher than the simply mixed colloid−bacterial suspension (Bacteria−AgNP). The total assay time of the presented method is only 10 min and a total reactants volume of merely 1 mL is required in a real-world sample, when measuring in the bulk liquid. When the analysis is performed by the new, hydrophobic glass surface approach, a droplet of only 3 μL sample is necessary for each analysis. Furthermore, we can use this novel strategy to discriminate three strains of *E. coli* and one strain of *S. epidermidis* by statistical methods. This method offers many advantages, such as reduced assay time, simple handling, lower reactant volumes, a small amount of sample, and higher sensitivity and selectivity compared to previously reported label free methods,[2,20,21,35] may be extended to open an avenue to develop various SERS-based biosensors.

■ ASSOCIATED CONTENT

Supporting Information

Zeta potential of *E. coli*; TEM characterizations of the silver nanoparticles; time-resolved SERS spectra of samples; tentative band assignment of the SERS spectra of the *E. coli*, and photo images and optical images of *E. coli*. This material is available free of charge via the Internet at http://pubs.acs.org.

■ AUTHOR INFORMATION

Corresponding Author

*C. Haisch. E-mail: Christoph.Haisch@ch.tum.de. Tel: +49 89 2180 78242. Fax: +49 89 2180 99 78242.

Notes

The authors declare no competing financial interest.

■ ACKNOWLEDGMENTS

Financial support by the China Scholarship Council (CSC) is gratefully acknowledged. We thank M. Seidel, K. Schwarzmeier and L. Pei for their help and advice, S. Mahler for technical support, C. Sternkopf for the ICP-MS analyses, and M. Hanzlik for the TEM measurements.

■ REFERENCES

(1) Fan, C.; Hu, Z. Q.; Mustapha, A.; Lin, M. S. *Appl. Microbiol. Biotechnol.* **2011**, *92*, 1053−1061.
(2) Walter, A.; Marz, A.; Schumacher, W.; Rosch, P.; Popp, J. *Lab Chip* **2011**, *11*, 1013−1021.
(3) Mead, P. S.; Slutsker, L.; Griffin, P. M.; Tauxe, R. V. *Emerging Infect. Dis.* **1999**, *5*, 841−842.
(4) Premasiri, W. R.; Moir, D. T.; Klempner, M. S.; Krieger, N.; Jones, G.; Ziegler, L. D. *J. Phys. Chem. B* **2005**, *109*, 312−320.
(5) Chu, H. Y.; Huang, Y. W.; Zhao, Y. P. *Appl. Spectrosc.* **2008**, *62*, 922−931.
(6) Deisingh, A. K.; Thompson, M. *Analyst (Cambridge, U. K.)* **2002**, *127*, 567−581.
(7) Kempf, V. A. J.; Mandle, T.; Schumacher, U.; Schafer, A.; Autenrieth, I. B. *Int. J. Med. Microbiol.* **2005**, *295*, 47−55.
(8) Dylla, B. L.; Vetter, E. A.; Hughes, J. G.; Cockerill, F. R. *J. Clin. Microbiol.* **1995**, *33*, 222−224.
(9) Belgrader, P.; Benett, W.; Hadley, D.; Richards, J.; Stratton, P.; Mariella, R.; Milanovich, F. *Science* **1999**, *284*, 449−450.
(10) Driskell, J. D.; Kwarta, K. M.; Lipert, R. J.; Porter, M. D.; Neill, J. D.; Ridpath, J. F. *Anal. Chem.* **2005**, *77*, 6147−6154.
(11) Fleischm, M.; Hendra, P. J.; McQuilla, A. J. *Chem. Phys. Lett.* **1974**, *26*, 163−166.
(12) Jeanmaire, D. L.; Vanduyne, R. P. *J. Electroanal. Chem.* **1977**, *84*, 1−20.
(13) Albrecht, M. G.; Creighton, J. A. *J. Am. Chem. Soc.* **1977**, *99*, 5215−5217.
(14) Zhou, H. B.; Zhang, Z. P.; Jiang, C. L.; Guan, G. J.; Zhang, K.; Mei, Q. S.; Liu, R. Y.; Wang, S. H. *Anal. Chem.* **2011**, *83*, 6913−6917.
(15) Wilson, R.; Bowden, S. A.; Parnell, J.; Cooper, J. M. *Anal. Chem.* **2010**, *82*, 2119−2123.
(16) Schlucker, S. *ChemPhysChem* **2009**, *10*, 1344−1354.
(17) Preciado-Flores, S.; Wheeler, D. A.; Tran, T. M.; Tanaka, Z.; Jiang, C. Y.; Barboza-Flores, M.; Qian, F.; Li, Y.; Chen, B.; Zhang, J. Z. *Chem. Commun.* **2011**, *47*, 4129−4131.
(18) Willets, K. A. *Anal. Bioanal. Chem.* **2009**, *394*, 85−94.
(19) Sun, L.; Sung, K. B.; Dentinger, C.; Lutz, B.; Nguyen, L.; Zhang, J. W.; Qin, H. Y.; Yamakawa, M.; Cao, M. Q.; Lu, Y.; Chmura, A. J.; Zhu, J.; Su, X.; Berlin, A. A.; Chan, S.; Knudsen, B. *Nano Lett.* **2007**, *7*, 351−356.
(20) Qian, X. M.; Peng, X. H.; Ansari, D. O.; Yin-Goen, Q.; Chen, G. Z.; Shin, D. M.; Yang, L.; Young, A. N.; Wang, M. D.; Nie, S. M. *Nat. Biotechnol.* **2008**, *26*, 83−90.
(21) Kahraman, M.; Zamaleeva, A. I.; Fakhrullin, R. F.; Culha, M. *Anal. Bioanal. Chem.* **2009**, *395*, 2559−2567.
(22) Jarvis, R. M.; Law, N.; Shadi, L. T.; O'Brien, P.; Lloyd, J. R.; Goodacre, R. *Anal. Chem.* **2008**, *80*, 6741−6746.
(23) Kahraman, M.; Keseroglu, K.; Culha, M. *Appl. Spectrosc.* **2011**, *65*, 500−506.
(24) Abell, J. L.; Garren, J. M.; Driskell, J. D.; Tripp, R. A.; Zhao, Y. P. *J. Am. Chem. Soc.* **2012**, *134*, 12889−12892.
(25) Drummond, T. G.; Hill, M. G.; Barton, J. K. *Nat. Biotechnol.* **2003**, *21*, 1192−1199.
(26) Jarvis, R. M.; Goodacre, R. *Anal. Chem.* **2004**, *76*, 40−47.
(27) Sztainbuch, I. W. *J. Chem. Phys.* **2006**, 125.
(28) Kahraman, M.; Yazici, M. M.; Sahin, F.; Bayrak, O. F.; Culha, M. *Appl. Spectrosc.* **2007**, *61*, 479−485.
(29) Kahraman, M.; Yazici, M. M.; Sahin, F.; Culha, M. *Langmuir* **2008**, *24*, 894−901.
(30) Berry, V.; Gole, A.; Kundu, S.; Murphy, C. J.; Saraf, R. F. *J. Am. Chem. Soc.* **2005**, *127*, 17600−17601.
(31) Berry, V.; Saraf, R. F. *Angew. Chem., Int. Edit* **2005**, *44*, 6668−6673.
(32) Wilson, W. W.; Wade, M. M.; Holman, S. C.; Champlin, F. R. *J. Microbiol. Methods* **2001**, *43*, 153−164.
(33) Efrima, S.; Bronk, B. V. *J. Phys. Chem. B* **1998**, *102*, 5947−5950.
(34) Zeiri, L.; Bronk, B. V.; Shabtai, Y.; Czege, J.; Efrima, S. *Colloid Surface. A* **2002**, *208*, 357−362.
(35) Zeiri, L.; Bronk, B. V.; Shabtai, Y.; Eichler, J.; Efrima, S. *Appl. Spectrosc.* **2004**, *58*, 33−40.
(36) Efrima, S.; Zeiri, L. *J. Raman. Spectrosc.* **2009**, *40*, 277−288.
(37) Wolter, A.; Niessner, R.; Seidel, M. *Anal. Chem.* **2007**, *79*, 4529−4537.
(38) Gao, D. M.; Wang, Z. Y.; Liu, B. H.; Ni, L.; Wu, M. H.; Zhang, Z. P. *Anal. Chem.* **2008**, *80*, 8545−8553.
(39) Schwarzmeier, K.; Knauer, M.; Ivleva, N. P.; Niessner, R.; Haisch, C. *Anal. Bioanal. Chem.* **2013**, *405*, 5387−5392.
(40) Knauer, M.; Ivleva, N. P.; Niessner, R.; Haisch, C. *Anal. Bioanal. Chem.* **2012**, *402*, 2663−2667.
(41) Knauer, M.; Ivleva, N. P.; Liu, X. J.; Niessner, R.; Haisch, C. *Anal. Chem.* **2010**, *82*, 2766−2772.
(42) Leopold, N.; Lendl, B. *J. Phys. Chem. B* **2003**, *107*, 5723−5727.
(43) Knauer, M.; Ivleva, N. P.; Niessner, R.; Haisch, C. *Anal. Sci.* **2010**, *26*, 761−766.
(44) Yang, L. B.; Liu, H. L.; Wang, J.; Zhou, F.; Tian, Z. Q.; Liu, J. H. *Chem. Commun.* **2011**, *47*, 3583−3585.
(45) Qian, K.; Yang, L. B.; Li, Z. Y.; Liu, J. H. *J. Raman. Spectrosc.* **2013**, *44*, 21−28.
(46) Li, J.; McLandsborough, L. A. *Int. J. Food Microbiol.* **1999**, *53*, 185−193.

(47) Xu, F. G.; Zhang, Y.; Sun, Y. J.; Shi, Y.; Wen, Z. W.; Li, Z. *J. Phys. Chem. C* **2011**, *115*, 9977−9983.